

Intense Electrical Pulsing of Perovskite Light Emitting Diodes under Cryogenic Conditions

Karim Elkhoully, Iakov Goldberg, Nirav Annavarapu, Robert Gehlhaar, Tung-Huei Ke, Jan Genoe, Johan Hofkens, Paul Heremans,* and Weiming Qiu*

As the threshold for stimulated emission is significantly reduced at cryogenic temperatures, cooling of perovskite light emitting diodes (PeLEDs) is considered an essential strategy for reaching injection lasing in perovskite diodes. In this work, we demonstrate the intense electrical pulsing of a PeLED stack up to a few kA cm^{-2} at cryogenic conditions. A high external quantum efficiency (EQE) of 2.9% at 1 kA cm^{-2} and a radiance $>1.95 \times 10^5 \text{ W Sr}^{-1} \text{ m}^{-2}$ are achieved when exciting the device with 250 ns electrical pulses at 77 K, showing three times enhancement in comparison with room temperature operation. Furthermore, we provide a comprehensive understanding on how the ion distribution can affect the PeLED characteristics and show that ion motions can be manipulated at cryogenic conditions. This opens new routes for novel material and device designs for further improving PeLED performance.

perovskite light emitting diode (PeLED) stack,^[11,12] and intense electrical excitation of PeLEDs up to several kA cm^{-2} current density.^[13–16]

Previous studies have shown that Joule heating is a detrimental factor that lowers the device performance at high current injection, even for small-scale PeLEDs excited with sub-microsecond electrical pulses.^[13,14,16] Therefore, the reduction of the device operating temperature has been considered as one of the key strategies that likely must be applied in order to achieve electrically pumped perovskite lasing.^[17] Moreover, cryogenic cooling of perovskite films and devices has also been shown to provide other benefits relevant for lasing, such as the exponential decrease in ASE threshold,^[4,8,18] freezing of nonradiative


recombination traps, higher device operational stability, etc.^[19] Furthermore, considering that ion migration/distribution plays a crucial role in determining the optoelectronic characteristics of PeLEDs,^[13,20,21] cryogenic cooling offers an opportunity to manipulate and freeze ion motions in the PeLED for an optimal device operation. However, despite the numerous advantages, intense electrical pulsing of PeLEDs under cryogenic conditions has not been studied yet, partially due to the scarcity of device stacks that can be properly operated at cryogenic temperatures.^[11] Moreover, a comprehensive understanding of the relationship between ion motion and electroluminescence (EL) output of PeLEDs under such measurement conditions is lacking. Therefore, addressing these questions can lead to new material and device engineering insights for the realization of an electrically pumped perovskite laser.

In this work, we propose a PeLED stack that maintains its electrical performance when cooled from RT down to 77 K. By investigating the temperature dependent PeLED characteristics in direct current (DC) operation, we show that the main device parameters such as the external quantum efficiency (EQE) and the current density–voltage–radiance (J – V – R) characteristics are dominated by the bias conditions during the cooling process. This observation allowed us to design experiments where the ions are manipulated through a combination of device cooling and DC bias. Then, by using microsecond electrical pulses at different temperatures, we were able to probe the effects of ion distribution on the PeLED characteristics. Finally, with this understanding, we were able to demonstrate an EQE of 2.9% at 1 kA cm^{-2} by applying short electrical pulses down to 250 ns to a miniaturized PeLED at 77 K. The PeLED also reaches a

1. Introduction

Metal-halide perovskites have attracted considerable attention as an exciting material system for future lasing applications, owing to their solution processibility and unique properties such as low amplified spontaneous emission (ASE) thresholds and high optical gain values.^[1–3] To date, optically pumped lasing has been routinely observed from perovskite films with various compositions.^[4–7] Nonetheless, the realization of an electrically pumped perovskite laser remains out of reach. Encouragingly, several important achievements toward this goal have been reported, in particular optically-pumped continuous-wave ASE/lasing in perovskite films at both cryogenic and room temperatures (RT),^[8–10] optically-pumped ASE from a complete

K. Elkhoully, I. Goldberg, N. Annavarapu, R. Gehlhaar, T.-H. Ke, J. Genoe, P. Heremans, W. Qiu
IMEC
Kapeldreef 75, Leuven 3001, Belgium
E-mail: Paul.Heremans@imec.be; Weiming.Qiu@imec.be
K. Elkhoully, I. Goldberg, N. Annavarapu, J. Genoe, P. Heremans
ESAT
KU Leuven
Kasteelpark Arenberg 10, Leuven 3001, Belgium
J. Hofkens, W. Qiu
Department of Chemistry
KU Leuven
Celestijnenlaan 200F, Leuven 3001, Belgium

 The ORCID identification number(s) for the author(s) of this article can be found under <https://doi.org/10.1002/adom.202200024>.

DOI: 10.1002/adom.202200024

radiance value $>195 \text{ kW Sr}^{-1} \text{ m}^{-2}$ at $J = 2.9 \text{ kA cm}^{-2}$, equivalent to a $J \cdot \text{EQE}$ product of 41 A cm^{-2} . Moreover, the device also retains 82% of its peak performance after $> 6 \times 10^5$ pulses when pulsed at 1 kA cm^{-2} at 77 K. Given that an order of magnitude reduction in the threshold carrier density for stimulated emission is expected at low temperatures,^[22] the demonstration of reliable kA cm^{-2} electrical pulsing under cryogenic conditions represents a crucial milestone for the realization of an electrically pumped perovskite laser.

2. Results and Discussion

We first investigate the optoelectronic characteristics of the PeLED at different temperatures under DC operation. The PeLED stack under investigation consists of Indium tin oxide (ITO)/ poly[N,N'-bis(4-butylphenyl)-N,N'-bis(phenyl)-benzidine] (PolyTPD)/ Formamidinium (FA), and Methylammonium (MA) dual-cation perovskite, i.e., $(\text{FAPbI}_3)_{0.95}(\text{MAPbBr}_3)_{0.05}/6,6'$ -phenyl-C₆₁-butyric acid methyl ester (PCBM)/ magnesium doped zinc oxide (ZnMgO)/ Aluminum (Al). The perovskite film is fabricated according to our previously reported procedure where 20 mol % of extra phenylmethylammonium iodide (PMAI) is added to form smooth crystalline films with passivated small grains.^[23] The layer thicknesses and the band diagram are shown in Figure S1 (Supporting Information).

Throughout all experiments, the PeLED is cooled down from RT to 77 K in a liquid nitrogen cryostat, and then the device is subsequently measured at increasing temperatures up to RT. At each temperature setpoint, we allow the device to settle for

30 min to reach the desired temperature. Figure 1a presents the EL spectra of our PeLED at different operating temperatures. With the decrease of temperature, the EL peaks are first systematically shifted to longer wavelengths, i.e., from 800 nm at RT to 820 nm at 125 K. However, the shift reverses direction when the PeLED is further cooled to 77 K, where it peaks at 815 nm. In contrast, the full width half maximum (FWHM) of the spectra monotonically narrows down from 40 nm at RT to 18 nm at 77 K. These trends are consistent with the previously reported results for FA-based PeLEDs.^[19] Importantly, as it is evident by the J - V characteristics in Figure 1b, although the driving voltage for the same current density rises at lower temperatures, this increase in driving voltage is significantly less than previous reports in the literature. For example, in our case, the voltage needed to reach 100 mA cm^{-2} only increases from 1.65 V at RT to 3.35 V at 77 K. For comparison, Kim et al. reported a device stack showing orders of magnitude deterioration in electrical conductivity at 110 K, due to increased series resistance stemming from the freeze-out of extrinsic carriers in the doped organic transport layer.^[11] More recently, He et al. reported an inverted PeLED that could reach current density of 100 mA cm^{-2} at a driving voltage of $\approx 6 \text{ V}$ at 65 K.^[19] Thus, our device shows superior carrier injection properties at cryogenic temperature, which is particularly important while aiming for lasing level current densities.

Aside from the good charge injection at low temperatures, we have also observed a notable difference in J - V characteristics and EL output when we cool down the device with and without a forward DC bias (we will refer to this condition as cooling down with DC bias throughout the manuscript, which

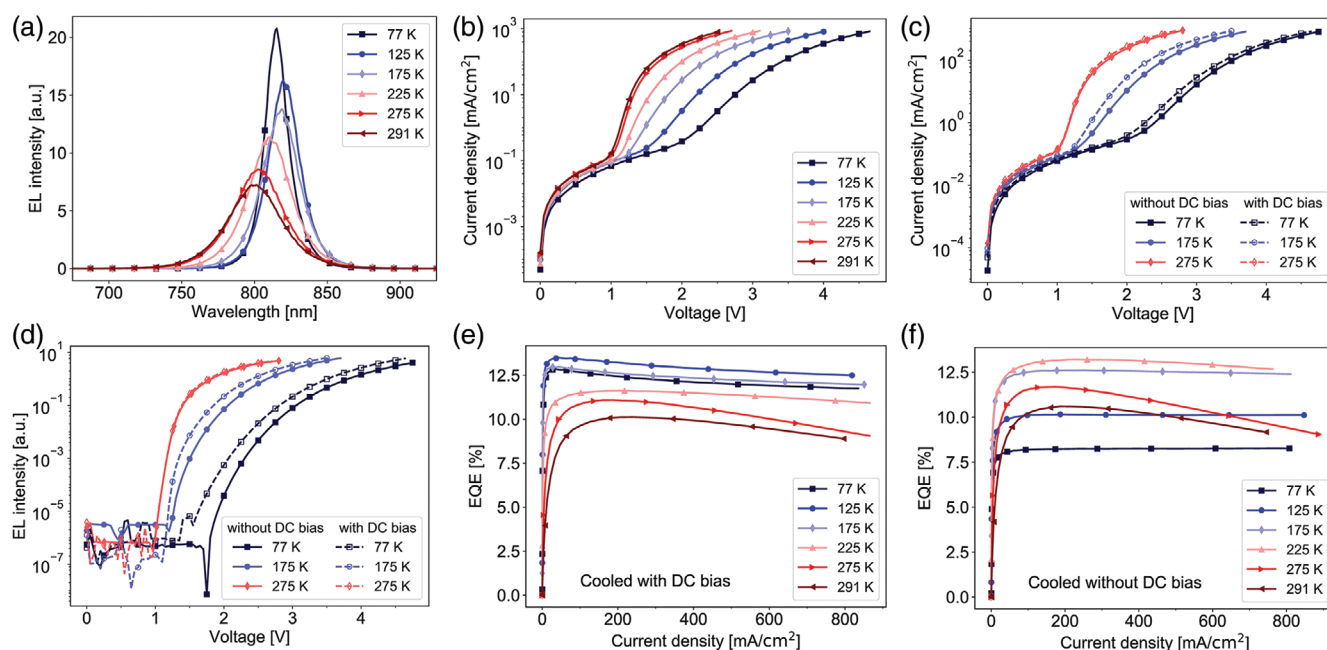


Figure 1. Optoelectronics characteristics of the PeLED at different temperatures. a) EL spectra measured at 100 mA cm^{-2} , the full-width half-maximum (FWHM) narrows down to 18 nm at 77 K. b) J - V curves showing systematic increase in the driving voltage with cooling. A comparison between the c) J - V curves and d) EL intensity- V curves when the PeLED is cooled down under a constant DC bias of 100 mA cm^{-2} (unfilled) and without DC bias (filled). The turn-on of light emission is shifted to higher voltages matching the increase in driving voltage at lower temperatures when the PeLED is cooled down without DC bias. EQE- J characteristics when the PeLED is cooled down e) under a constant DC bias of 100 mA cm^{-2} , and f) without DC bias. The EQE- J plots at different temperatures show significant variation depending on the bias conditions during cooling.

corresponds to cooling down with the PeLED under a constant current density of 100 mA cm^{-2}). By comparing the J - V curves in Figure 1c, it is clear that the curves obtained from the same device that was initially cooled without DC bias shift to higher voltages at lower temperatures, as represented by the cases of 77 and 175 K. Nevertheless, this voltage shift, which can be as large as 0.3 V, diminishes at higher temperatures. At 275 K, we can observe that the two curves overlap, with no dependence on the device initial cooling condition. Consistently, the turn-on voltage, defined as the onset of light emission in the EL intensity- V plot in Figure 1d also systematically shifts to higher voltages when the PeLED is cooled down without a DC bias. It is noteworthy that the change of EL spectra with temperature shows the same trend disregarding whether we cool the device with or without DC bias (Figure S2, Supporting Information).

In our previous work, we have shown that ion motions in PeLEDs result in slow transients for current and EL on a sub-second to second or even longer timescale, which remarkably modifies the carrier injection behavior and recombination dynamics.^[20,24] Thus, Ion migration and the final ion distribution determine the device characteristics.^[20,21] In the current case, considering that even the most mobile ionic species have relatively high activation energies in the range of 100–300 meV,^[25,26] ion migration in the PeLED is expected to be extensively slowed down or even frozen at low temperature. Therefore, at 77 or 175 K, the mobile ions cannot quickly relax back to their initial positions upon the removal of DC bias applied during cooling. Hence, it is expected that cooling the PeLED with or without DC bias leads to a completely different ion distribution within the device. This can well explain the different J - V curves measured at such temperatures. On the contrary, the ions are free to relax at 275 K upon the removal of DC bias, resulting in the same ion distribution as that in the case of cooling without bias and the overlapping J - V curves. Furthermore, such influence of cooling condition on the corresponding ion distribution is also reflected in the strikingly different EQE- J plots shown in Figure 1e,f. Although for both cooling conditions, we can obtain a peak EQE of 10.5% at RT which then reaches a maximum of 13.2% upon device cooling, the temperature at which the maximum EQE is achieved is remarkably different. The maximum EQE is reached at 125 K in the case of cooling with DC bias, but at 225 K when no DC bias is applied during cooling. Moreover, at 77 K, the PeLED cooled without bias achieves a peak EQE of only 8.3%, compared to 12.8% when the PeLED is cooled with bias.

To provide further evidence for the freezing of ion distribution at low temperatures, impedance spectroscopy measurements were done at different temperatures on the same PeLED (Figure S3a, Supporting Information). We observe that the low frequency capacitance at RT is dominated by ionic contributions.^[25] However, the ionic component is strongly suppressed by cooling down the device and is nearly frequency independent at 77 K. Similar conclusions are reached by measuring the transient response of the EL intensity when a constant bias of 100 mA cm^{-2} is applied to the device at different temperatures (Figure S3b, Supporting Information). It is noted that while the EL intensity signal undergoes a slow transient at high temperatures, sharp transients are observed at low temperatures, consistent with the freezing of ion motion at low temperatures.

These results demonstrate that the optoelectronic characteristics of the PeLED are not only governed by the intrinsic carrier dynamics of the perovskite materials, i.e., nonradiative recombination rate, radiative recombination rate, etc., but are also significantly affected by the ion distribution within the device. Interestingly, at low temperature, we can temporarily freeze the ion distribution profile by slowing down ion motions. This opens a novel way for reaching the optimal PeLED performance through manipulating the ion distribution.

The above results with DC bias indicate that it is possible to alter the PeLED performance through ion manipulation. However, under DC excitations, the ions cannot be completely frozen during the measurements. Indeed, we will show later in this section that a DC electric field can move the ions even at low temperature. To have a better control of the mobile ions and to give a clearer picture of their roles in determining device performance, we use pulsed electrical excitation at different temperatures. Typically, ions in PeLEDs move on a timescale of milliseconds to seconds and cannot respond to fast electrical pulses.^[13] Therefore, by using electrical pulses in the microsecond timescale with a very low duty cycle, one can probe the electrical characteristics of the PeLED without significantly affecting the ion distribution. In essence, we can use a DC bias to establish a certain ion distribution profile and temporarily freeze it at cryogenic temperature, then use microsecond electrical pulses to probe the device characteristics without disturbing the ions. Moreover, with pulsed electrical excitation, one can also measure to much higher current density without degrading the PeLED.

To begin with, we carried out experiments similar to the ones done in DC, i.e., performing measurements on the same PeLED cooled with and without a DC bias. However, in this case, microsecond electrical pulses are used instead of DC excitation. The J - V curves recorded from the pulsed operation at different temperatures are shown in Figure S4 (Supporting Information). Similar to the observation in DC excitations, the driving voltage increases at lower temperatures. We note that the series resistance of the ITO electrode dominates the diode resistance at voltages $>10 \text{ V}$, where the curves overlap. We first focus on the investigation of the EQE- J characteristics, which are shown in Figure 2a,b. For the case where the device is cooled without DC bias (Figure 2a), we observe that the peak EQE of 7.7% remains the same for the temperature range between 77 and 175 K. This is in stark contrast to the above DC measurements on the same device shown in Figure 1f, where the peak EQE increases with temperature from 77 to 225 K. Furthermore, at temperatures $>175 \text{ K}$, the peak EQE measured with microsecond pulses keeps decreasing and approaches a mere 5% at RT. This value is about half of that attained from the DC measurements and is achieved at current densities significantly higher than those measured in DC. Both differences mentioned above can be explained by the fact that during the DC measurements the ion distribution is actively changed by the voltage sweep, while in the pulsed measurement the ions cannot respond to the fast electrical pulses. Since ion re-arrangement is required to facilitate the charge injection and shift the recombination zone away from the perovskite/transport layers interfaces,^[13,20] lower EQE values are expected when we measure the PeLED cooled without DC bias using the pulsed excitation rather than the DC excitation.

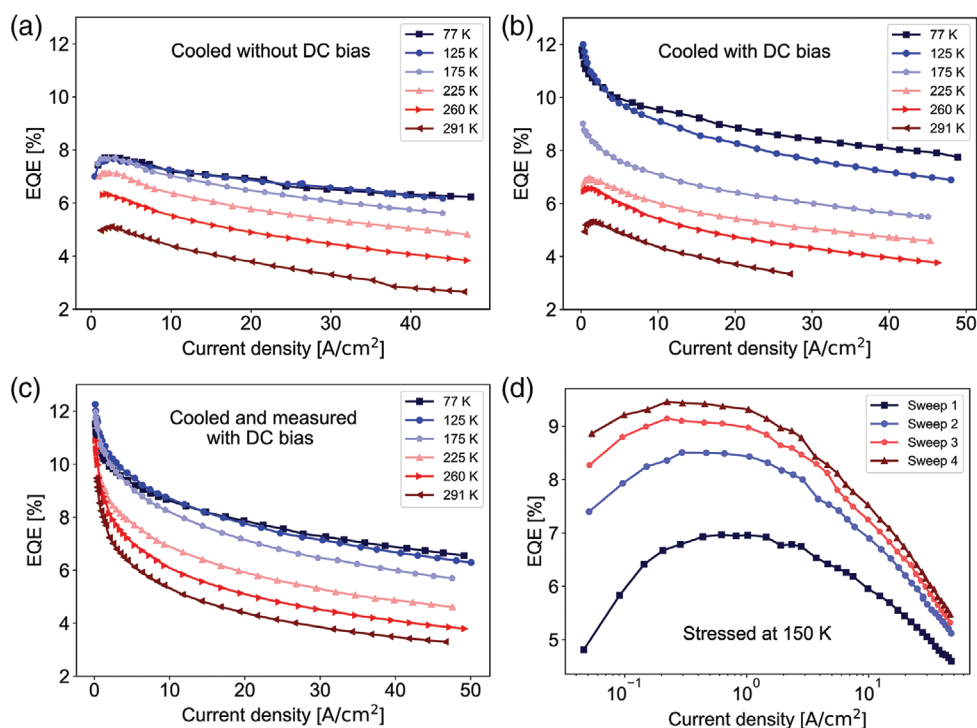


Figure 2. Pulsed EQE- J characteristics of the PeLED at different temperatures and bias conditions. a) The PeLED is cooled down without DC bias. b) The PeLED is cooled down under a constant DC bias of 100 mA cm^{-2} . c) The PeLED is cooled down and measured under a constant DC bias of 100 mA cm^{-2} . d) The PeLED is cooled down to 150 K without the application of DC bias and consequently measured using microsecond electrical pulses (sweep 1). The PeLED is then stressed at 200 mA cm^{-2} for 15 min for three times, and is measured after each stressing cycle using the same microsecond-pulsing protocol (sweeps 2–4).

For the case where the PeLED is cooled with DC bias, we can again get a peak EQE of 12% at 77 K (Figure 2b), similar to the value obtained from the DC measurement in Figure 1e. Moreover, compared to the case of cooling without DC bias, the recorded EQE values are significantly higher in the temperature range from 77 to 175 K. It is also noted that the peak EQE is achieved at low current densities, in contrast to the cooling without DC bias case. These observations are due to the more favorable ion distribution realized by the DC bias during cooling. In the temperature range from 225 to 291 K, the EQE- J plots under the pulsed excitation seem virtually independent of the application of a DC bias during initial cooling to 77 K. This indicates that the ion distribution, established by cooling the device with DC bias to 77 K, can gradually relax as the temperature is increased when the DC bias is removed. Especially, above 175 K, the ion distribution can relax fully to a similar profile to the case of cooling without DC bias. To validate this point, we have further measured the same device cooled with DC bias under pulsed excitation but also with DC background bias. In other words, the DC bias applied during device cooling is kept in place also during the pulsed measurements. It can be observed in Figure 2c that the use of background bias significantly enhances the EQE values obtained at temperatures above 175 K, reaching peak EQE values similar to that from DC excitation. In contrast, the background bias shows much less influence on the EQE- J plot measured at 77 K.

The above investigation demonstrated that: 1) it is possible to temporarily freeze a certain ion distribution profile in a PeLED at low temperature without further relaxation to equilibrium positions by virtue of the remarkably slower ion motions; 2) DC bias can still move the mobile ions even at low temperatures. This means that one can use a DC bias to tailor the ion distribution at low temperature. Based on such understanding, we have designed an experiment to study the effect of gradual ion migration at low temperature. First, the PeLED is cooled down without DC bias to 150 K. Then, microsecond electrical pulses are used to probe the optoelectronic characteristics of the PeLED (noted as sweep 1). Following this measurement, the PeLED is stressed at a constant bias of 200 mA cm^{-2} for 15 min to move the ions, and after removing the constant bias another measurement is performed with microsecond electrical pulses (noted as sweep 2). Such protocols are repeated for another two times, resulting in sweep 3 and sweep 4. In this way, we can gradually change the ion distribution within the device. From the EQE- J plot presented in Figure 2d, it is clear that the gradual change in ion distribution leads to a progressive increase in EQE values, yielding almost a factor of two improvement in the peak EQE between sweep 4 and sweep 1.

Apart from the EQE- J characteristics, the corresponding transient electroluminescence (TransEL) curves also provide valuable insight into the operation mechanism of the PeLED. Figure 3a exhibits the normalized TransEL curves recorded at 77 K for the condition where the PeLED is cooled without DC

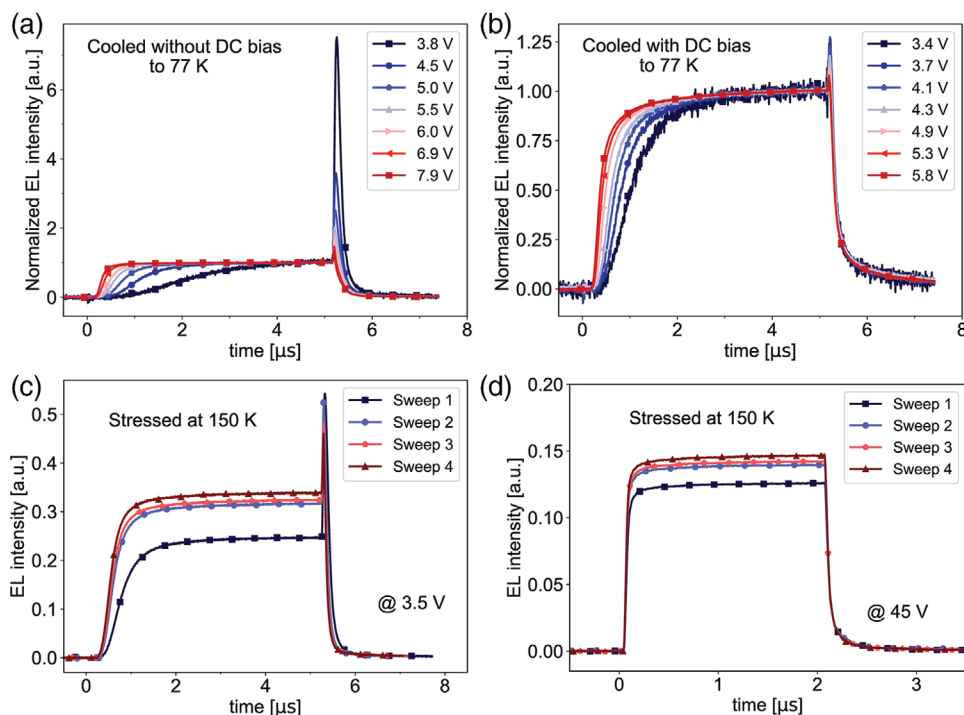


Figure 3. Normalized TransEL pulses of the PeLED at 77 K at different voltages for a) PeLED cooled down without DC bias and b) PeLED cooled down with constant DC bias of 100 mA cm^{-2} . The pulses are normalized by the stabilized EL at the end of each pulse. c,d) TransEL pulses at 150 K when the PeLED is cooled down without DC bias, and then stressed at 200 mA cm^{-2} for 15 min for three successive times. The TransEL pulses are shown for an applied voltage of c) 3.5 V, and d) 45 V.

bias. For each curve, the intensity is normalized by that of the stabilized EL before the end of the pulse. The unnormalized curves are shown in Figure S5 (Supporting Information). The most distinctive feature is the overshoot effect, which appears after the termination of the voltage pulse. The intensity of such overshoot reaches more than six times of the stabilized EL value at the end of the pulse at a relatively low pulsing voltage of 3.8 V. With an increase of pulsing voltage, the overshoot effect diminishes. The EL overshoot has been previously observed in thin-film optoelectronic devices based on organics,^[27] quantum dots,^[28] and perovskites. Gegevičius et al. have modeled and verified this effect in a typical perovskite solar cell at RT, showing that the mixing of charge carriers that were accumulated near the transport layer/perovskite interfaces is responsible for this phenomenon.^[29]

Cooling the PeLED with DC bias severely quenches the overshoot effect, as shown in Figure 3b. In this case, the intensity of the overshooting peak is restricted to <25% increase over the stabilized EL intensity. This result points to the critical role of ion distribution in the overshoot phenomenon. Further evidence can be found by investigating the TransEL curves corresponding to the experiment shown in Figure 2d, in which the PeLED was stressed multiple times with DC bias at 150 K and subsequently measured after each stressing. Figure 3c plots the four TransEL curves taken at a voltage pulse of 3.5 V after each stressing. On one hand, these TransEL curves illustrate a monotonic enhancement in the stabilized EL intensity after each stressing cycle, which is reflected in the EQE enhancement shown in Figure 2d. On the other hand, this increase is

accompanied by a systematic reduction in the overshoot effect after each stressing cycle. These results indicate the rearrangement of the ions reduces the charge carrier accumulation near the transport layer/perovskite interfaces. Notably, while inspecting the TransEL curves measured at a high voltage pulse of 45 V instead of 3.5 V, we could not observe the overshoot effect (Figure 4d). This indicates the negligible role of ion-induced carrier accumulation at high bias conditions. Nonetheless, the stabilized EL intensity is still appreciably enhanced after each stressing.

In addition to our demonstration of the possibility to systematically shift ion distribution at low temperatures, our results show that applying a constant background DC bias is a universal approach to increase EQE in pulsed mode. This observation has already been reported by Kim et al. in a different PeLED stack.^[13] To demonstrate the generality, we further fabricated a different PeLED stack based on methylammonium lead iodide (MAPbI₃). By sending microsecond electrical pulses at different background DC bias conditions, we observe a monotonic increase in the EQE for higher DC biases (Figure S6a, Supporting Information). The increase is drastic at low current density $<1 \text{ A cm}^{-2}$, exceeding an order of magnitude enhancement when the DC bias is increased from 0 to 1.9 V. However, the EQE-*J* plots converge at higher currents showing much lower enhancement factor, likely because the EQE roll-off at higher current density is dominated by other mechanisms. Moreover, the pulsed *J-V* characteristics (Figure S6b, Supporting Information) give higher current densities at the same voltage for larger background DC biases, which is consistent with our

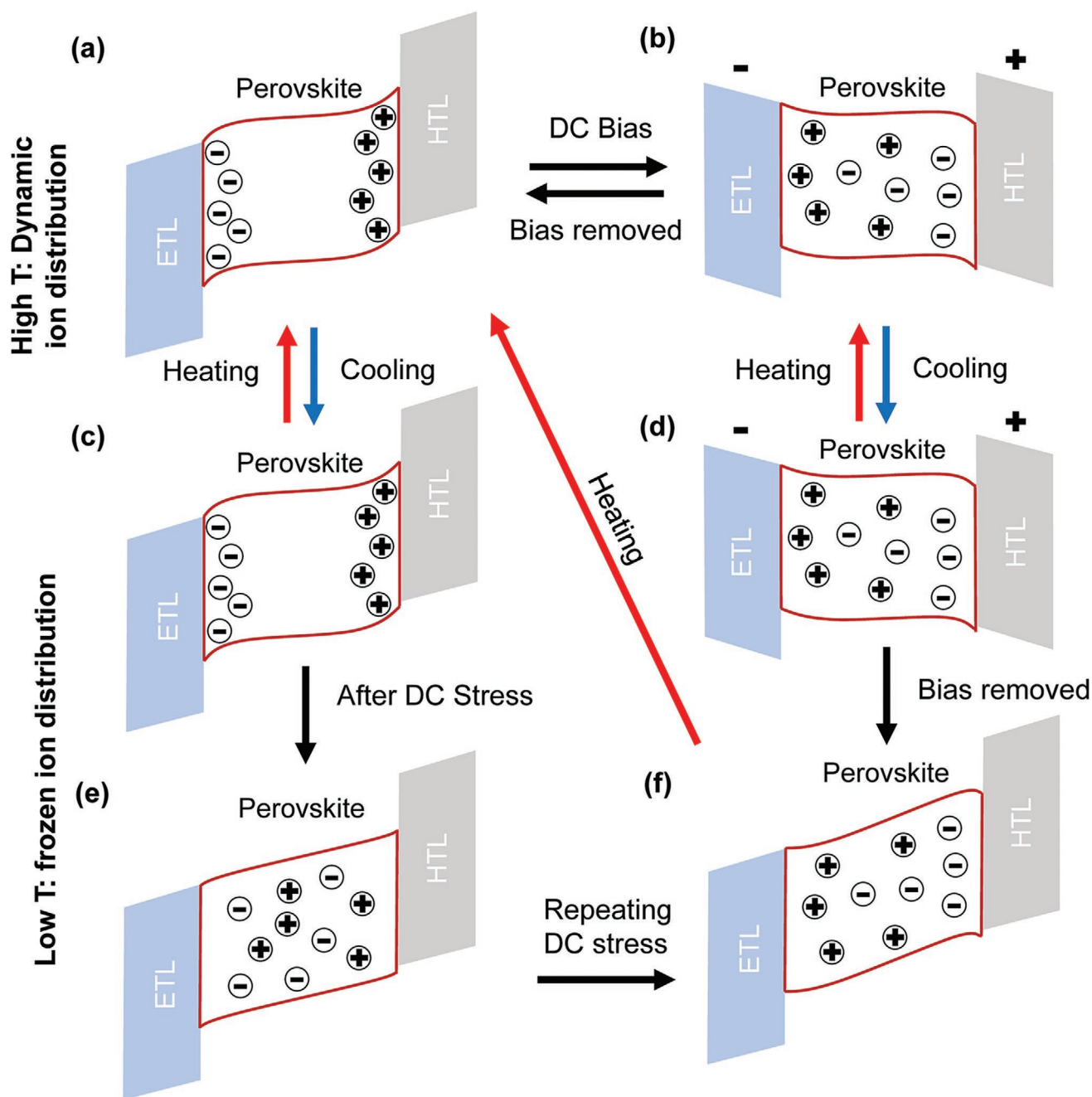


Figure 4. Model for PeLED cooling and ion migration. a) At equilibrium, the built-in electric field accumulates positive and negative ions at the perovskite/hole transport layer (HTL) and the perovskite/ETL interfaces, respectively. This ion distribution induces an energy barrier for carrier injection, partially screens the built-in electric field and favors carrier recombination close to the interfaces. b) After the application of a large forward DC bias, ions drift under the influence of the electric field to the opposite interface, leading to a more uniform, or even reversed ion distribution. A steady state distribution is reached after sufficient electrical stress. However, when the DC bias is removed, ions drift back to the equilibrium distribution under the influence of the built-in electric field. c) Cooling down the PeLED without DC bias freezes the equilibrium ion distribution, while d) cooling down the PeLED with DC bias freezes the stressed ion distribution. e) Continuous DC stressing at low temperature gradually changes the ion distribution, however, ions do not migrate back to the equilibrium distribution after removing the DC bias because the ion motions are slowed down at low temperature. f) A temporarily frozen stressed ion distribution can be achieved at low temperature through cooling down the PeLED with DC bias or by DC stressing at low temperatures.

observations for the FA-based PeLED studied in this work. By repeating the experiment for a different PeLED employing TPBi/LiF electron transport layer (ETL) instead of PCBM/ZnMgO, we

observe a similar increase for higher background biases confirming the generality of this observation for different stacks and transport layers (Figure S6c, Supporting Information). It

is noteworthy that by cooling the TPBi/LiF devices to lower temperatures, we get a similar trend in EQE enhancement. However, the electrical conductivity of the stack deteriorates compared to room temperature performance (Figure S7b, Supporting Information), demonstrating the important role played by the PCBM/ZnMgO ETL in maintaining good electrical performance at low temperatures.

The results discussed above can be summarized by a unified model shown in Figure 4, which extends the PeLED models previously reported in the literature.^[13,20,29] In our previous work, we have shown through activation energy measurements that the dynamic performance of our PeLEDs is likely dominated by iodine negative ions and positive vacancies.^[20] Initially, at RT in equilibrium (Figure 4a), due to the built-in electric field, negative and positive ions are accumulated at electron and hole transport layer interfaces, respectively, leading to band bending at the interfaces. Not only does it form an energy barrier for carrier injection, but it also concentrates the injected carriers primarily at the different interfaces, which is detrimental to the radiative recombination.^[13,20] When a forward DC bias is applied, these ions previously accumulated at the interfaces are drifted toward the opposite side, reversing the equilibrium ion distribution (Figure 4b). This will significantly facilitate charge injection and make radiative recombination more efficient. However, when the DC bias is removed at RT, ions can quickly relax to their initial equilibrium distribution in Figure 4a with the help of the built-in electric field. Now, if the PeLED is cooled down without a DC bias, a similar ion distribution to the one shown in Figure 4a will remain (Figure 4c). However, if the PeLED is cooled down with a DC bias (Figure 4d), the device will have a similar ion distribution as that presented in Figure 4b. Furthermore, such ion distribution can be kept even though the bias is removed after the cooling process (Figure 4f), since the ion motion is slowed down at low temperature, as demonstrated by impedance spectroscopy and transient EL measurements in Figure S3 (Supporting Information). This explains the pronounced performance improvement when the device is cooled with a DC bias at low temperature. Then, if the PeLED is heated up without a DC bias, a transition from Figure 4f to Figure 4a will happen, due to relaxation of ions at an elevated temperature. Therefore, the performance recorded at temperature range from 225 to 291 K is identical in Figure 2a,b. On the contrary, if the PeLED is heated up with a DC bias, represented by the transition from Figure 4d to Figure 4b, there will be negligible change in ion distribution, explaining the results that we measured with background DC bias. Finally, we can gradually move the ions using a DC bias at low temperature, making a transition from Figure 4c to Figure 4e. By repeating the DC bias or by using a prolonged DC bias, we can again achieve the ion distribution shown in Figure 4f.

The same model can be used to explain the overshoot effects as well. In equilibrium, ion accumulation at the interfaces induces a band bending that facilitates the accumulation of charge carriers and in turn results in an EL overshoot (Figure 4c). However, cooling the PeLED under a DC bias eliminates the band bending that quenches the overshoot effect. The same explanation applies to the situation when the PeLED is successively stressed with a DC bias at low temperature (Figure 4e). Finally, we note that the EL overshoot cannot be

observed at high current densities irrespective of the cooling and bias conditions. It is likely that ion-induced band-bending that leads to carrier accumulation is only relevant for certain ionic profiles at low carrier densities, while at high current densities, carriers are not localized in these locations, and are possibly leaking out of device contributing to EQE roll-off observed in all measurements.

Our model clearly shows the important role played by the ions in enhancing the EQE achieved under electrical excitation. This intrigues the question whether inhibiting ion migration would ultimately be beneficial to the PeLED performance. It is worth noting that although ion migration is understood to be a defect-mediated process,^[30,31] the performance enhancement due to ion migration is observed even in the state-of-the-art PeLEDs with an EQE approaching 20%, which is close to the outcoupling limit. Despite the low trap density, Kumuat et al. observed an order of magnitude enhancement in EL intensity when the pulse width is increased from 100 μ s to 1 ms.^[21] Since it is almost inevitable to have excess ions in perovskite films where those ions can accumulate at the interfaces due to the built-in electric field, this leads to injection barriers and band bending at the interfaces. Particularly for high-performance PeLEDs, extra ligands are commonly added as defect passivator, which introduces excess ions to the perovskite films. An interesting question is whether a hypothetical mobile ion-free device would perform better or worse than the PeLED studied in this work. On the one hand, our model suggests that the band-bending and the energy barriers induced at equilibrium due to excess ions reduce device performance. Therefore, in absence of excess ions, PeLED performance should improve from the electrostatics perspective and be more stable with electrical pulsing. On the other hand, we have also shown that when the mobile ions are located at the proper positions, the device performance can be enhanced. Therefore, mobile ions can be a double-edged sword, and it is important to manipulate the ion distributions in the PeLED.

We have so far focused on understanding the operating mechanisms for pulsing the PeLED at cryogenic temperatures. Based on this understanding and by making miniaturized devices, we were able to reach high EQE at current density in the range of kA cm^{-2} that is relevant for achieving injection lasing. A scaled circular PeLED with a diameter of 200 μ m was fabricated according to our previously reported procedure,^[16] where a silicon nitride dielectric layer was used to define the active device area. From the DC characteristics measured at different temperatures (Figure S8, Supporting Information), our miniaturized device shows very similar device characteristics to the PeLED studied in Figure 1.

To measure the device under intense pulsed excitation, we have used variable pulse widths ranging between 2 μ s and 250 ns. Furthermore, to maximize the EL output in the pulsed excitation, the miniaturized PeLED is first cooled down under a constant DC bias of 100 mA cm^{-2} and then measured without removing this background bias. Figure 5a illustrates the TransEL curves recorded at different current densities at 77 K, while the curves for the corresponding voltage and current pulses are shown in Figure S9 (Supporting Information). The variable pulse width allows the PeLED to reach stabilized EL intensity, i.e., a flat plateau in the EL output, for different

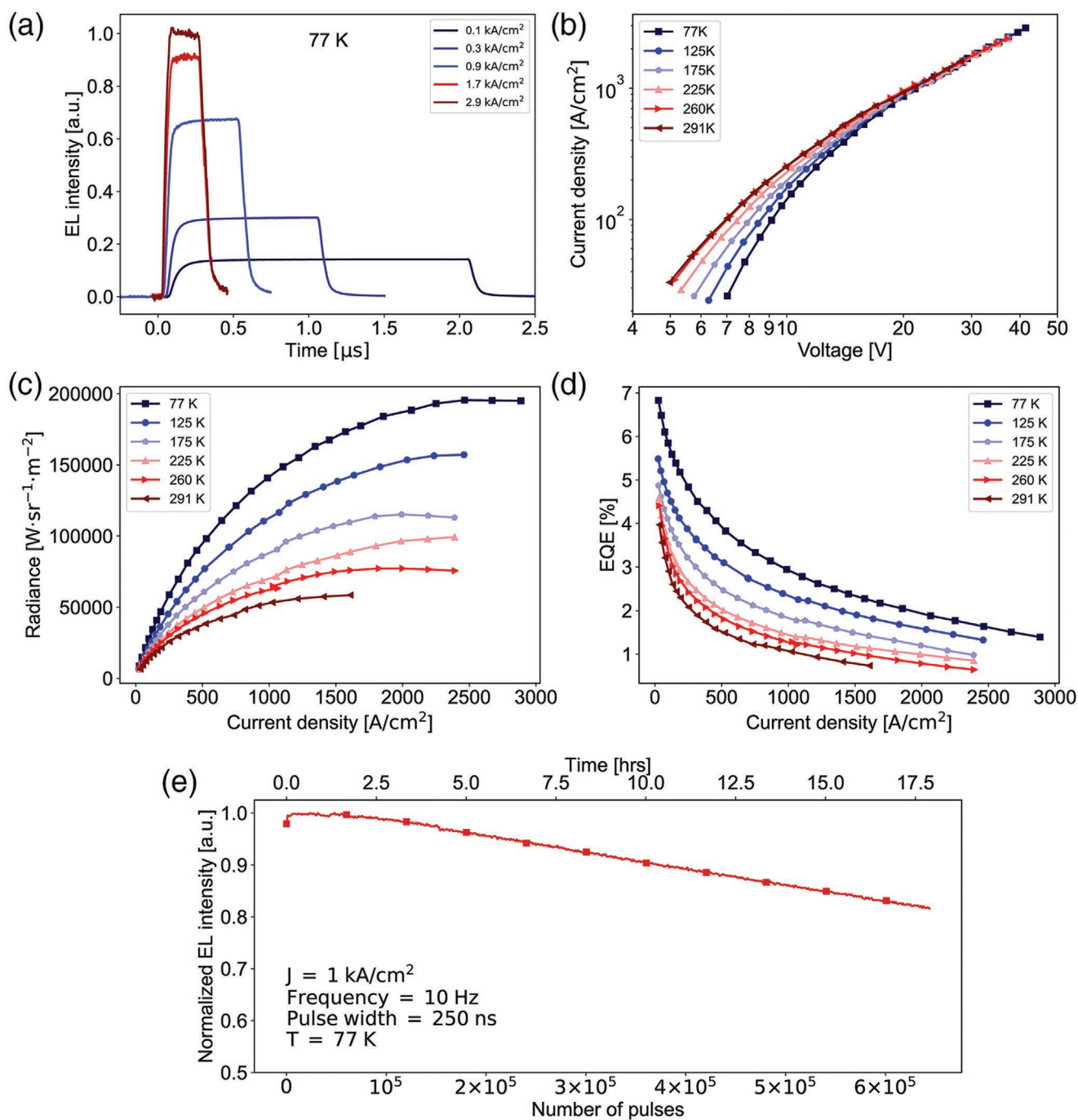


Figure 5. Optoelectronic characteristics of the miniaturized PeLED under intense electrical pulsing at different temperatures. a) TransEL pulse of variable pulse widths at different current densities at 77 K. b) J - V characteristics and c) R - J characteristics at different temperatures. The plots shift to higher voltages at lower temperatures; however, ITO series resistance dominates at higher currents, while radiance values reach $>195 \text{ kW Sr}^{-1} \text{ m}^{-2}$. d) EQE- J characteristics at different temperatures. EQE is significantly enhanced at lower temperatures, achieving 2.9% at 1 kA cm^{-2} . e) Stability test under 1 kA cm^{-2} pulsed excitation at 77 K.

current densities. It requires relatively longer pulses to get such a plateau at low current densities due to the longer rise time, but at high current densities short pulses are needed to mitigate the effect of Joule heating during measurement. However, at extreme current densities, the Joule heating induced EL decay cannot be avoided at all temperatures even for pulse widths as

short as 250 ns (Figure S10, Supporting Information). It is also noteworthy that the TransEL pulse shapes do not show any significant temperature dependence, confirming the excellent electrical characteristics of our PeLED at all measured temperatures.

Based on the curves recorded for the current density and TransEL at different temperatures, we plotted the J - V , R - J ,

and EQE- J characteristics of the miniaturized PeLED. From the J - V plot (Figure 5b), we can again observe that the curves shift toward higher voltages with the temperature decrease in the relatively lower current density range. However, the injected current density becomes independent of temperature at voltages over 20 V, or a corresponding current density over 800 A cm⁻². Under these circumstances, the resistance of the PeLED is dominated by the ITO series resistance that is largely temperature-independent. Most importantly cryogenic cooling significantly enhances the EL output, with the maximum radiance increasing from $\approx 5.8 \times 10^4$ W Sr⁻¹ m⁻² at RT to $>1.95 \times 10^5$ W Sr⁻¹ m⁻² at 77 K. Therefore, we can demonstrate a stabilized EQE of 2.9% at 1 kA cm⁻² at 77 K (vs. 0.9% at RT) as well as a J -EQE product of 41 A cm⁻² at 2.5 kA cm⁻² (Figure 5d). This is in the vicinity of the estimated value needed to achieve electrically pumped ASE.^[13,14] To study the effect of bias conditions on the PeLED performance at kA cm⁻² current densities, we cooled the same PeLED with a DC bias; however, the measurements were repeated without using a background DC bias at different temperatures (Figure S11, Supporting Information). Consistently with the measurements for the bigger device discussed in Figure 2b,c, there is a close overlap between both experiments at the lowest temperatures of 77 and 125 K, showing that the ionic distribution is frozen. However, starting from 175 K, we observe a discrepancy between the EQE plot for the two experiments pointing to the fact that the ionic distribution is relaxing, where the experiment based on a background DC bias during measurement gives higher EQEs. This shows that ion migration plays a critical role in carrier injection and charge balance even at extreme current densities >1 kA cm⁻². Finally, to demonstrate the reliability of pulsing our PeLED at extreme current densities at 77 K, we measure the stability of the miniaturized device at a current density of 1 kA cm⁻². The PeLED shows remarkable stability, retaining 82% of its peak performance after $> 6 \times 10^5$ pulses with a pulse width of 250 ns (Figure 5e). Interestingly, by repeating the cooling cycle and re-measuring the PeLED under similar excitation conditions. We observe that the PeLED generally recovers most of its peak performance. This might be related to the self-repairing effect in PeLEDs (Figure S12, Supporting Information).^[32]

Although the dominant mechanism behind EQE roll-off in PeLEDs at different temperatures remains unclear, our study allows us to conclude that Joule heating, which appears as a decay in the TransEL pulse at all temperatures (Figure S10, Supporting Information), plays a minimal role up to current densities as high as 1 kA cm⁻² for our device layout and pulsing conditions. On the contrary, our demonstration of the important role played by ion migration in determining the EQE of the PeLED shows that charge balance plays a critical role in determining the device performance, even at current densities as high as several kA cm⁻². Finally, it is important to note that other EQE roll-off mechanisms such as Auger recombination and electric-field induced quenching remain unexplored in this study.

3. Conclusion

In conclusion, we have demonstrated PeLEDs that maintain excellent electrical performance at cryogenic temperatures,

allowing us to study their optoelectronics characteristics under such circumstances. Through multiple experiments, we have provided a comprehensive understanding of the working mechanism of PeLED at different temperatures in relation to ion migration. In particular, we show an effective way to manipulate the ions with DC bias and temporarily freeze the ion distribution at low temperatures. With the help of microsecond electrical pulses, this offers an interesting opportunity to investigate the effects of ion migration on the PeLED optoelectronic characteristics without disturbing the ion distribution. The fact that we can manipulate ions at cryogenic temperatures opens new routes for novel material and device design. Then, by optimizing intense electrical pulsing at cryogenic temperatures, we have achieved a high EQE of 2.9% at 1 kA cm⁻² at 77 K, which corresponds to a factor three enhancement compared to that of RT. The significance of this result is that it has become apparent from the literature that electrically pumped lasing in PeLEDs will require operation at cryogenic temperatures. Indeed, to date, continuous wave ASE in 3D perovskites was only shown at temperatures <160 K.^[8,9,22] Furthermore, operation at cryogenic temperatures also exponentially lowers the ASE threshold.^[4,8,18] Therefore, our results demonstrate that intense pulsing at cryogenic temperatures is a promising strategy for a proof-of-concept demonstration of an electrically pumped perovskite laser.

Supporting Information

Supporting Information is available from the Wiley Online Library or from the author.

Acknowledgements

The authors acknowledge funding from the European Research Council under the European Horizon 2020 Programme/ERC grant agreement no. 835133 (ULTRA-LUX). W.Q. would like to thank the financial support of the postdoctoral fellowship grant from FWO (1252322N). J.H. gratefully acknowledges financial support from the Research Foundation – Flanders (FWO Grant Numbers S002019N, 1514220N, G098319N, and ZW15_09-GOH6316), the KU Leuven Research Fund (iBOF-21-085 PERSIST) and the Flemish government through long term structural funding Methusalem (CASAS2, Meth/15/04).

Conflict of Interest

The authors declare no conflict of interest.

Data Availability Statement

The data that support the findings of this study are available from the corresponding author upon reasonable request.

Keywords

cryogenic, electrical pulsing, ion migration, lasing, overshoot

Received: January 5, 2022

Revised: March 25, 2022

Published online: May 4, 2022

- [1] B. R. Sutherland, E. H. Sargent, *Nat. Photonics* **2016**, *10*, 295.
- [2] L. N. Quan, B. P. Rand, R. H. Friend, S. G. Mhaisalkar, T.-W. Lee, E. H. Sargent, *Chem. Rev.* **2019**, *119*, 7444.
- [3] L. Lei, Q. Dong, K. Gundogdu, F. So, *Adv. Funct. Mater.* **2021**, *31*, 2010144.
- [4] Y. Jia, R. A. Kerner, A. J. Grede, A. N. Brigeman, B. P. Rand, N. C. Giebink, *Nano Lett.* **2016**, *16*, 4624.
- [5] S. Chen, K. Roh, J. Lee, W. K. Chong, Y. Lu, N. Mathews, T. C. Sum, A. Nurmikko, *ACS Nano* **2016**, *10*, 3959.
- [6] C.-Y. Huang, C. Zou, C. Mao, K. L. Corp, Y.-C. Yao, Y.-J. Lee, C. W. Schlenker, A. K. Y. Jen, L. Y. Lin, *ACS Photonics* **2017**, *4*, 2281.
- [7] N. Pourdavoud, T. Haeger, A. Mayer, P. J. Cegielski, A. L. Giesecke, R. Heiderhoff, S. Olthof, S. Zaefferer, I. Shutsko, A. Henkel, D. Becker-Koch, M. Stein, M. Cehovski, O. Charfi, H. H. Johannes, D. Rogalla, M. C. Lemme, M. Koch, Y. Vaynzof, K. Meerholz, W. Kowalsky, H. C. Scheer, P. Gorrn, T. Riedl, *Adv. Mater.* **2019**, *31*, 1903717.
- [8] P. Brenner, O. Bar-On, M. Jakoby, I. Allegro, B. S. Richards, U. W. Paetzold, I. A. Howard, J. Scheuer, U. Lemmer, *Nat. Commun.* **2019**, *10*, 988.
- [9] Y. Jia, R. A. Kerner, A. J. Grede, B. P. Rand, N. C. Giebink, *Nat. Photonics* **2017**, *11*, 784.
- [10] C. Qin, A. S. D. Sandanayaka, C. Zhao, T. Matsushima, D. Zhang, T. Fujihara, C. Adachi, *Nature* **2020**, *585*, 53.
- [11] H. Kim, K. Roh, J. P. Murphy, L. Zhao, W. B. Gunnarsson, E. Longhi, S. Barlow, S. R. Marder, B. P. Rand, N. C. Giebink, *Adv. Opt. Mater.* **2020**, *8*, 1901297.
- [12] C. Cho, T. Antrack, M. Kroll, Q. An, T. R. Bärschneider, A. Fischer, S. Meister, Y. Vaynzof, K. Leo, *Adv. Sci.* **2021**, *8*, 2101663.
- [13] H. Kim, L. Zhao, J. S. Price, A. J. Grede, K. Roh, A. N. Brigeman, M. Lopez, B. P. Rand, N. C. Giebink, *Nat. Commun.* **2018**, *9*, 4893.
- [14] L. Zhao, K. Roh, S. Kacmoli, K. Al Kurdi, S. Jhulki, S. Barlow, S. R. Marder, C. Gmachl, B. P. Rand, *Adv. Mater.* **2020**, *32*, 2000752.
- [15] L. Zhao, K. Roh, S. Kacmoli, K. Al Kurdi, X. Liu, S. Barlow, S. R. Marder, C. Gmachl, B. P. Rand, *Adv. Mater.* **2021**, *33*, 2104867.
- [16] I. Goldberg, W. Qiu, K. Elkhoully, N. Annavarapu, A. N. Mehta, C. Rolin, T. H. Ke, R. Gehlhaar, J. Genoe, P. Heremans, *J. Mater. Chem. C* **2021**, *9*, 12661.
- [17] W. B. Gunnarsson, B. P. Rand, *APL Mater.* **2020**, *8*, 030902.
- [18] I. Allegro, Y. Li, B. S. Richards, U. W. Paetzold, U. Lemmer, I. A. Howard, *J. Phys. Chem. Lett.* **2021**, *12*, 2293.
- [19] Y. He, J. Yan, L. Xu, B. Zhang, Q. Cheng, Y. Cao, J. Zhang, C. Tao, Y. Wei, K. Wen, Z. Kuang, G. M. Chow, Z. Shen, Q. Peng, W. Huang, J. Wang, *Adv. Mater.* **2021**, *33*, 2006302.
- [20] J. Chmeliov, K. Elkhoully, R. Gegevičius, L. Jonušis, A. Devižis, A. Gelžinis, M. Franckevičius, I. Goldberg, J. Hofkens, P. Heremans, W. Qiu, V. Gulbinas, *Adv. Optical Mater.* **2021**, *9*, 2101560.
- [21] N. K. Kumawat, W. Tress, F. Gao, *Nat. Commun.* **2021**, *12*, 4899.
- [22] Y. Jia, R. A. Kerner, A. J. Grede, B. P. Rand, N. C. Giebink, *Adv. Opt. Mater.* **2020**, *8*, 1901514.
- [23] K. Elkhoully, I. Goldberg, H. Boyen, A. Franquet, V. Spampinato, T. Ke, R. Gehlhaar, J. Genoe, J. Hofkens, P. Heremans, W. Qiu, *Adv. Optical Mater.* **2021**, *9*, 2100586.
- [24] K. Elkhoully, R. Gehlhaar, J. Genoe, P. Heremans, W. Qiu, *Adv. Optical Mater.* **2020**, *8*, 2000941.
- [25] M. H. Futscher, J. M. Lee, L. McGovern, L. A. Muscarella, T. Wang, M. I. Haider, A. Fakharuddin, L. Schmidt-Mende, B. Ehrler, *Mater. Horiz.* **2019**, *6*, 1497.
- [26] J.-W. Lee, S.-G. Kim, J.-M. Yang, Y. Yang, N.-G. Park, *APL Mater.* **2019**, *7*, 041111.
- [27] V. R. Nikitenko, V. I. Arkhipov, Y.-H. Tak, J. Pommerehne, H. Bässler, *J. Appl. Phys.* **1997**, *81*, 7514.
- [28] Q. Shen, Y. Hao, L. Ma, X. Wang, *J. Phys. Chem. Lett.* **2021**, *12*, 7019.
- [29] R. Gegevičius, M. Franckevičius, J. Chmeliov, W. Tress, V. Gulbinas, *J. Phys. Chem. Lett.* **2019**, *10*, 1779.
- [30] C. Eames, J. M. Frost, P. R. Barnes, B. C. O'regan, A. Walsh, M. S. Islam, *Nat. Commun.* **2015**, *6*, 7497.
- [31] A. Senocrate, I. Spanopoulos, N. Zibouche, J. Maier, M. S. Islam, M. G. Kanatzidis, *Chem. Mater.* **2021**, *33*, 719.
- [32] P. Teng, S. Reichert, W. Xu, S. C. Yang, F. Fu, Y. Zou, C. Yin, C. Bao, M. Karlsson, X. Liu, J. Qin, T. Yu, W. Tress, Y. Yang, B. Sun, C. Deibe, F. Gao, *Matter.* **2021**, *4*, 3710.